HHS Public Access

Author manuscript

Nat Chem Biol. Author manuscript; available in PMC 2010 August 01.

Published in final edited form as:

Nat Chem Biol. 2010 February ; 6(2): 109–116. doi:10.1038/nchembio.284.

Substrate-dependent proton antiport in neurotransmitter:sodium symporters

Yongfang Zhao[1,7], **Matthias Quick**[1,2,4,7], **Lei Shi**[5,6], **Ernest L. Mehler**[5], **Harel Weinstein**[5,6], and **Jonathan A. Javitch**[1,2,3,4,*]

[1]Center for Molecular Recognition, Columbia University College of Physicians and Surgeons, 630 W. 168th, New York, New York 10032, USA.

[2]Department of Psychiatry, Columbia University College of Physicians and Surgeons, 630 W. 168th, New York, New York 10032, USA.

[3]Department of Pharmacology, Columbia University College of Physicians and Surgeons, 630 W. 168th, New York, New York 10032, USA.

[4]Division of Molecular Therapeutics, New York State Psychiatric Institute, New York, NY 10032, USA.

[5]Department of Physiology and Biophysics, Weill Medical College of Cornell University, 1300 York Avenue, New York, NY 10021, USA.

[6]HRH Prince Alwaleed Bin Talal Bin Abdulaziz Alsaud Institute for Computational Biomedicine, Weill Medical College of Cornell University, 1300 York Avenue, New York, NY 10021, USA

SUMMARY

Neurotransmitter:sodium symporters (NSS), targets for psychostimulants and therapeutic drugs, play a critical role in neurotransmission. Whereas eukaryotic NSS exhibit Cl^--dependent transport, bacterial NSS feature Cl^--independent substrate transport. Recently we showed in LeuT and Tyt1 that mutation of an acidic side chain near one of the Na^+-binding sites renders substrate binding and/or transport Cl^- dependent. We reasoned that the negative charge - provided either by Cl^- or by the transporter itself - is required for substrate translocation. Here we show that Tyt1 reconstituted in proteoliposomes is strictly dependent on the Na^+ gradient and is stimulated by an inside negative membrane potential and by an *inversely-oriented* H^+ gradient. Remarkably, Na^+/substrate symport elicited H^+ efflux, indicative of Na^+/substrate symport-coupled H^+ antiport. Mutations that render the transport phenotype Cl^--dependent essentially abolish the pH

*Columbia University College of Physicians and Surgeons, Center for Molecular Recognition, 630 West 168th Street, P&S 11-401, New York, NY 10032, USA; Phone: 212-305-3974; Facsimile: 212-305-5594; jaj2@columbia.edu.

[7]these authors contributed equally

AUTHOR CONTRIBUTION Y.Z. and M.Q. designed and performed transport and binding studies; L.S. and E.L.M. designed, carried out, and analyzed the computational simulations and pKa calculations. H.W. and J.A.J. helped to design experiments and analyze data related to the computational and biochemical studies, respectively. M.Q., L.S., E.L.M., H.W., and J.A.J. contributed to writing and editing the manuscript.

The authors declare no competing financial interests.

dependence. We propose unifying features of charge balance by all NSS members with similar mechanistic features but with different molecular solutions.

Members of the eukaryotic neurotransmitter:sodium symporter (NSS) family play an essential role in the nervous system by terminating synaptic transmission and recycling various neurotransmitters, including biogenic amines and amino acids1. The transporters for the biogenic amines dopamine (**1**), norepinephrine (**2**), and serotonin (**3**), (DAT, NET, SERT, respectively) are of particular interest because they are the primary targets for widely abused psychostimulant drugs such as cocaine (**4**) and amphetamine(**5**)2, and for antidepressants3. These secondary active transporters catalyze the (re)-uptake of their respective substrates from the extracellular milieu against their concentration gradient across the plasma membrane of presynaptic neurons4-6 in a cotransport (symport) mechanism driven by the Na^+ electrochemical gradient7, 8. Several members of the prokaryotic NSS family have been identified, namely TnaT9, LeuT10, Tyt111, and MhsT12. These amino acid transport systems, like their eukaryotic counterparts, exhibit a strict Na^+ dependence; however, in contrast to the Cl^--dependence of most eukaryotic NSS, all of the prokaryotic NSS studied to date are Cl^- independent9-13.

Recently, we showed that introducing a negatively charged amino acid at or near one of the two Na^+-binding sites of the GABA (**6**) transporter GAT1 (S331→E) renders substrate transport Cl^- independent, whereas the reciprocal mutations in LeuT and Tyt1 result in Cl^--dependent substrate binding and/or transport13. Interestingly, whereas GAT1-wild-type transport activity is pH independent, GABA transport in the Cl^--independent GAT1 mutant (S331E) is markedly stimulated by acidic internal pH13. We hypothesized that the carboxyl side chain of E introduced in place of S331 can bind and unbind H^+ during the transport cycle and that in Cl^--independent NSS, H^+ may be counter-transported, i.e. by a Na^+/substrate-coupled H^+ antiport mechanism, to facilitate the return step of the “empty” transporter13. Indeed, we also observed a pH-dependent substrate transport phenotype for Tyt1-wild-type (WT) in *E. coli* 11 and when reconstituted into proteoliposomes12. Since both the electrical membrane potential ($\Delta\Psi$) and the chemical gradient of ions across the membrane (i.e. $\Delta\mu_{Na^+}$ or $\Delta\mu_{H^+}$) contribute to the distribution of conformational states of a transporter14, we sought to analyze the effect of membrane potential and ionic composition on Na^+-coupled Tyr (**7**) symport by Tyt1 reconstituted in proteoliposomes. In this system, artificial ion gradients ($\Delta\tilde{\mu}_{Na^+}$ or $\Delta\mu_{H^+}$) can be imposed across the proteoliposome membrane by varying the internal and external buffer composition, and a membrane potential ($\Delta\Psi$; inside negative) can be created by an outward-directed K^+ diffusion gradient in the presence of valinomycin (**8**).

Here we report that the activity of Tyt1 and another Cl^--independent bacterial homolog of the NSS family, MhsT, is dependent on the Na^+ gradient and is stimulated by membrane potential (inside negative), and an inversely-oriented H^+ gradient. Remarkably, we identify a heretofore unknown H^+ flux that is coupled to Na^+/substrate symport, consistent with a Na^+/substrate symport/H^+ counter-transport mechanism.

RESULTS

Cl^- and pH-dependent tyrosine uptake in intact *E. coli*

In a recent study13 we have shown the importance of the charge of the amino acid side chains at position 7.38 or 7.42 (N327 and S331 in GAT1, respectively; for indexing system see15, 16) for the distinction between Cl^--dependent and Cl^--independent transport (Supplementary Table 1). Whereas the Cl^--dependent members of the NSS family possess neutral amino acids at those positions, Cl^--independent NSS members have a negatively charged amino acid at either position. Figure 1a shows the effect of replacing NaCl with Na-gluconate (**9**) on the time course of Na^+-dependent Tyr transport by intact *E. coli* expressing Tyt1 variants. Whereas Tyt1-WT exhibited no significant difference between the uptake of 1 μM ^{3}H-Tyr in the presence of 10 mM NaCl (3935 ± 176 pmol × mg^{-1} × min^{-1}) or Na-gluconate (3741 ± 238 pmol × mg^{-1} × min^{-1}), the Cl^--dependent mutant Tyt1-D259$^{7.38}$N/A263$^{7.42}$N mediated transport only when Cl^- was present (with an initial rate of 42.4 ± 6.2 pmol × mg^{-1} × min^{-1}; Fig. 1a, Inset). In the presence of Na-gluconate the activity of this mutant was indistinguishable from that observed in control cells lacking recombinant Tyt1. Despite the significant activity of Tyt1-D259N/A263N in the presence of 100 mM NaCl, the initial rate of transport and the steady state of Tyr accumulation was only ~ 1 % and ~ 10 %, respectively, of that determined for Tyt1-WT at the given test conditions.

Tyt1-WT exhibited initial rates of 1 μM ^{3}H-Tyr uptake that were greatly dependent on the external pH with a peak at pH 8.5, regardless of whether the assay was performed in the presence of NaCl or Na-gluconate (Fig. 1b). Initial rates for Tyt1-WT-mediated Tyr uptake varied between ~ 150 pmol Tyr × min^{-1} × mg of total cell $protein^{-1}$ at pH 6.5 and ~ 2500 pmol Tyr × min^{-1} × mg of total cell $protein^{-1}$ at pH 8.5. In striking contrast, for Tyt1-D259N/A263N we observed significantly reduced initial rates of 1 μM ^{3}H-Tyr transport in the presence of 100 mM NaCl (about 30 pmol Tyr × min^{-1} × mg of total cell $protein^{-1}$), and these rates were independent of pH over the entire range tested. A change in the external pH also had no effect on the transport activity by Tyt1-D259N/A263N in the presence of Na-gluconate; it was only about 20 % of that observed in the presence of NaCl.

Fig. 1c shows the effect of increasing NaCl concentrations on the initial rate of Tyr transport by Tyt1-WT (left panel) and the Cl^--dependent Tyt1 mutant (right panel). In an attempt to improve transport we introduced a third mutation in the Cl^- site, T260$^{7.39}$N to make the sequence more similar to that of the Cl^--dependent NSS members. Combining the D259N/A263N mutations in Tyt1 with T260N resulted in a transporter construct with an enhanced expression level in *E. coli* or *L. lactis*, but with other properties nearly identical to the double mutant D259N/A263N (data not shown); consequently, this mutant was used for all subsequent studies. Testing the effect of increasing NaCl concentrations (≤ 50 mM) on the uptake activity of Tyt1-WT revealed an apparent $K_{0.5}^{Na^+}$ of 1 ± 0.1 mM with a Hill coefficient of 1.5 ± 0.2, consistent with previous results11. NaCl concentrations > 50 mM resulted in inhibition of Tyr transport in intact *E. coli*, similar to observations in other Na^+-dependent symport proteins17. Tyr transport by Tyt1-D259N/T260N/A263N exhibited a ~100-fold increase in the apparent $K_{0.5}^{Na^+}$ (92 ± 9.4 mM; Hill coefficient of 1.5 ± 0.2 mM [data fit from 0 – 400 mM]; Fig. 1c, right panel). Note, however, that the calculated $K_{0.5}^{Na^+}$

substantially underestimates the true $K_{0.5}^{Na^+}$ of this mutant due to the superimposed effect of high Na^+ concentrations inhibiting Tyr uptake, as evident in Tyt1-WT.

Uptake kinetics of Tyt1 in proteoliposomes

Expression of recombinant Tyt1 in *L. lactis* cells and its subsequent purification12 yielded highly pure full-length transporter as judged by protein-analytical techniques (Supplementary Fig. 1 online). Proteoliposomes made from preformed liposomes that were destabilized with Triton X-100 at the onset of solubilization and reconstituted with purified Tyt1 at a protein-to-lipid ratio of 1:200 (w/w) showed the highest transport activity among the conditions tested (Supplementary Fig. 2 online) and were used for all subsequent studies. The Na^+-dependence of Tyt1-mediated Tyr transport into proteoliposomes was confirmed by measuring the time course of 1 μM ^{3}H-Tyr in the presence or absence of 25 mM NaCl (Fig. 2a). Diluting proteoliposomes with an internal buffer composition of 100 mM KP_i, pH 6.5 into 50 mM Tris/Mes, pH 8.5 in the presence of 25 mM NaCl (generation of $\Delta\tilde{\mu}_{Na^+}$ and *negative* $\Delta\mu_{H^+}$ [$pH_{in} < pH_{out}$]) resulted in an initial rate of Tyr transport (180 ± 12 nmol × min^{-1} × mg of $Tyt1^{-1}$) that was ~570 times higher than that in the absence of Na^+ (equimolar replacement with Tris/Mes). Consistent with our previous observation of severely reduced Tyr uptake by the Cl^--dependent Tyt1-D259N/T260N/A263N in intact *E. coli*, reconstitution of this mutant into proteoliposomes produced only about 1 % of the initial rate of ^{3}H-Tyr transport catalyzed by Tyt1-WT in the presence of 25 mM NaCl (Fig. 2b). Note that in contrast to the whole-cell measurements described above in *E. coli*, these data reflect the protein-specific activity, i.e. secondary effects of other intrinsic membrane proteins in *E. coli* that may account for the effects reported above can be ruled out. The activity of Tyt1-WT was indistinguishable when measured in NaCl or Na-gluconate. In contrast, transport by reconstituted Tyt1-D259N/T260N/A263N was chloride dependent, as we demonstrated previously in intact *E. coli*13 - in Na-gluconate ^{3}H-Tyr accumulation was similar to that observed in control liposomes.

Whereas Tyt1-WT in proteoliposomes exhibited a similar apparent $K_{0.5}^{Na^+}$ as observed in *E. coli*12, Na^+-stimulated ^{3}H-Tyr uptake in Tyt1-D259N/T260N/A263N-containing proteoliposomes did not reach saturation at the highest NaCl concentration tested (400 mM; Fig. 2c), consistent with our results in intact *E. coli* cells (Fig. 1c, right panel).

Next, we tested whether $\Delta\mu_{H^+}$ is sufficient as the sole driving force of tyrosine transport (Fig. 2d). Tyt1-WT-containing proteoliposomes were created in the presence of 25 mM NaCl at pH 6.5 or pH 7.5. Dilution of these proteoliposomes in 25 mM external NaCl ($\Delta\tilde{\mu}_{Na^+}=0$) resulted in Tyr uptake activity that was indistinguishable from the activity observed in control liposomes under the same experimental conditions, regardless of whether the direction of $\Delta\mu_{H^+}$ was inward or outward. Likewise, in the absence of $\Delta\mu_{Na^+}$ the generation of a valinomycin-mediated $\Delta\Psi$ (in the presence or absence of $\Delta\mu_{H^+}$ in either direction) resulted in Tyr uptake by Tyt1-WT identical to that observed in control liposomes (data not shown).

Figure 3a shows the effect of an inwardly-directed membrane potential ($\Delta\Psi$) on Na^+-coupled Tyr transport in the absence of a pH difference across the liposome membrane (pH_{in}

= pH_{out} = 6.5; $\Delta\mu_{H^+} = 0$). The initial rate of Na^+-driven transport (determined after 10 seconds) was 9.4 ± 2.4 nmol Tyr × min^{-1} × mg $Tyt1^{-1}$. This rate was increased almost 2-fold (18.1 ± 3.9 Tyr × min^{-1} × mg $Tyt1^{-1}$) when a K^+ diffusion membrane potential was generated by the addition of valinomycin. In the presence of gramicidin, which dissipated $\Delta\mu_{Na^+}$, the accumulation of ^{3}H-Tyr in Tyt1-containing proteoliposomes was indistinguishable from that observed in control liposomes (not shown). In contrast to the result obtained in Fig. 3a, a valinomycin-induced outwardly-directed membrane potential (−ΔΨ) blunted Na^+-coupled Tyr transport (Fig. 3b) even under optimized $\Delta\mu_{H^+}$ conditions (pH_{in} = 6.5, pH_{out} = 8.5; see Fig. 3c).

We performed a systematic comparison of the effect of $\Delta\mu_{H^+}$ on the $\Delta\tilde{\mu}_{Na^+}$-driven transport reaction across the liposome membrane (Fig. 3c). Transport increased with increasing pH_{out} and decreasing pH_{in}, yielding the highest value (250.9 ± 15.9 nmol Tyr × mg $Tyt1^{-1}$ × min^{-1}) at pH_{in} of 6.5 and pH_{out} of 8.5.

According to our hypothesis13, the negatively charged side chain of aspartate/glutamate 7.38 or 7.42 has to be protonated for the reorientation step of the transporter. If this proton was released to the extracellular milieu upon reorientation of the transporter, H^+ antiport would be associated with Na^+ symport and the transport cycle would be accelerated by an outward H^+ gradient. Indeed, although $\Delta\mu_{H^+}$ did not drive Tyr transport in the absence of $\Delta\mu_{Na^+}$ (Fig. 2c), the initial rate of Na^+-dependent Tyr transport by Tyt1-WT in proteoliposomes with an internal pH of 6.5 was increased by about 500 % when the external pH was raised from 6.5 to 8.5 (Fig. 3c). The same qualitative increase was observed at an internal pH of 7.5 and 8.5, but to a lesser extent (see Fig. 3c in which the transport rates are shown). In contrast, under the same experimental conditions Tyt1-D259N/T260N/A263N-mediated Tyr transport was maximally stimulated only to about 80 %. This result clearly demonstrates the combined effects of ΔΨ, $\Delta\mu_{Na^+}$, and negative $\Delta\mu_{H^+}$ on Tyt1-WT-mediated substrate transport, whereas the $\Delta\mu_{H^+}$ effect is absent or blunted in the Cl^--dependent mutant.

Different binding and uptake kinetics

To assess the substrate binding properties of the individual Tyt1 variants, we performed equilibrium binding studies by means of scintillation proximity12. In striking contrast to ^{3}H-Tyr flux measurements, binding of 1 μM ^{3}H-Tyr to purified Tyt1-WT and to Tyt1-D259N/T260N/A263N was pH-independent over a range from pH 6.5 to 9.0 (Fig. 4a). This result suggests that the H^+ dependence of uptake occurs at a step in the cycle after substrate binding. ^{3}H-Tyr bound to purified Tyt1-WT and -D259N/T260N/A263N with a similar K_D^{Tyr} of 5.8 ± 0.8 μM and 8.4 ± 1.7 μM, respectively, when measured in the presence of 200 mM NaCl at pH 7.5. Higher NaCl concentrations did not exert an inhibitory effect on the equilibrium binding activity of Tyt1-WT (data not shown), and the apparent $K_D^{Na^+}$ was ~ 90 mM as we showed previously12. In contrast, binding of 1 μM ^{3}H-Tyr to Tyt1-D259N/T260N/A263N did not saturate at NaCl concentrations as high as 400 mM (data not shown).

The apparent affinity of Tyr uptake ($K_{0.5}^{Tyr}$) in proteoliposomes with an internal pH of 6.5 remained the same (~ 0.5 μM) when the external pH was varied between 6.5 and 8.5 (Fig. 4b). Consistent with the notion of protonation of the transporter being required for maximum substrate flux, increasing the external pH in those experiments from 6.5 to 8.5 resulted in a ~ 6-fold increased maximum velocity of Tyr transport (V_{max}^{Tyr} of 48 ± 5.1, 253 ± 11.8, and 292 ± 8.1 nmol × mg Tyt1^{-1} × min^{-1} at pH_{out} 6.5, 7.5, and 8.5, respectively), and, in turn, in the turnover number of transport (k_{trsp} = 0.04 ± 0.004 × s^{-1}, 0.2 ± 0.01 × s^{-1}, and 0.25 ± 0.007 × s^{-1}). Similar to the reduced initial rates of Tyr transport in whole-cell measurements (Fig. 1), at 200 mM NaCl the Cl^--dependent/pH-independent Tyt1-variant D259N/T260N/A263N exhibited a ~ 62-fold reduced velocity of transport (V_{max}^{Tyr}=5 ± 0.3 $nmol \times mg \quad Tyt1^{-1} \times min^{-1}$; k_{trsp} = 0.004 ± 0.0002 × s^{-1})) and a ~9-fold increased $K_{0.5}^{Tyr}$ (4.9 ± 0.8 μM), compared to Tyt1-WT (Fig. 4c).

Internal pH changes in response to Na^+-coupled substrate transport

Given the stimulating effect of a negative $\Delta\mu_{H^+}$ on substrate transport by Tyt1 reconstituted in proteoliposomes, we speculated that Na^+-dependent substrate symport by Tyt1 is coupled to H^+ antiport. To test this hypothesis we measured substrate-induced intra-compartmental pH changes using fluorescent probes. Significant ligand-induced changes in the 5(6)-carboxyfluorescein succinimidyl ester (cFSE) fluorescence intensity ratio, indicative of alkalization of the cytoplasm, were detected in *L. lactis* NZ9000 expressing recombinant Tyt1 but not in control cells (Fig. 5a). Small, albeit consistent fluorescence changes were observed when only the co-transported cation Na^+ was added to the cell solution, but the simultaneous addition of Na^+ and Tyr led to the largest signal. Similar results were observed when another bacterial NSS homolog, MhsT, a Na^+-dependent hydrophobic amino acid transporter of the alkaliphilic *B. halodurans*12 was expressed in *L. lactis* (Fig. 5b). The cytoplasmic alkalization reached saturation within ~2 min upon the addition of Na^+ and Tyr, consistent with the time course of ^{3}H-Tyr transport mediated by Tyt1 (Fig. 1a and 2a).

To validate our findings in a cell-free system, we measured changes in pyranine fluorescence in proteoliposomes reconstituted with purified Tyt1 (Fig. 5c). Significant alkalization of the proteoliposomes' lumen was observed when Na^+ and Tyr were added together, and, to a smaller extent when Tyr was added in the nominal absence of Na^+ (Fig. 5c, left panel). Rapid alkalinization was also observed upon addition of Na^+ and Tyr in the presence of the K^+ ionophore valinomycin (Supplementary Fig. 3 online), excluding the possibility that H^+ extrusion results from the accumulation of positive charge in the lumen of the proteoliposomes due to the electrogenic nature of Tyt1 function. In contrast, no significant changes were detected upon addition of the substrates to control liposomes devoid of Tyt1 or to proteoliposomes containing Tyt1-D259N/T260N/A263N (Fig. 5c, right panel). While this is consistent with the lack of H^+ antiport in this mutant, we cannot rule out the possibility that the low transport activity of this mutant makes it impossible to observe changes in the fluorescence.

To obtain an estimate of the coupling stoichiometry of Na^+/Tyr symport-coupled H^+-translocation we calculated $V_{max}^{H^+}$ (maximum velocity of H^+ translocation; see SUPPLEMENTARY

METHODS) of three independent experiments (51.3 ± 2.3 nmol H^+ × (mg Tyt1 × min)$^{-1}$) and compared it with the V_{max}^{Tyr} obtained in Tyt1-containing proteoliposomes at $pH_{in} = pH_{out}$ = 7.5 (38.4 ± 0.6 nmol Tyr × (mg Tyt1 × min)$^{-1}$). Under those experimental conditions, the H^+-to-Tyr coupling ratio was calculated to be 1.34 ± 0.06. Note, however, that this estimate is based on a number of approximations of liposome size and geometry (see SUPPLEMENTARY METHODS). [Au: Appropriate to call out Supplementary Methods in both instances in this paragraph, as we do not allow callouts to Supplementary Information?]

Function-related conformational rearrangements modulate the pKa of E290 in LeuT (D259 in Tyt1)

The structural rearrangement associated with opening the "cytoplasmic gate" of the protein to enable release of Na^+ and substrate to the intracellular milieu changes the local environment around E290 and greatly increases the penetration of water into the permeation pathway18. To understand the consequences of these changes in the local environment produced by the modeled conformational rearrangement, we carried out comparative pKa calculations using the MM_SCP approach19 and molecular models of LeuT and Tyt1 embedded in lipid bilayer membranes. The molecules were either in the crystal structure-like conformation, or in the modeled inward-facing conformations derived from our intracellular-pulling Steered Molecular Dynamics (SMD) study18. Comparing the pKa obtained from the calculated acid/base equilibrium of E290 in the crystal structure-like conformation of LeuT (pKa = 3.6) to that in the inward-facing model (pKa = 6.9) shows that the conformational change associated with transport produces a very significant increase in the propensity for the protonated state of the acidic side chain. Similar results were obtained for the D259 of Tyt1 (pKa values of 2.7 and 6.4, respectively). These results support our interpretation of the observed pH effect on transport.

Analysis of the mechanism producing the calculated changes in the pKa values demonstrates how the pH dependence is integrated in the functional mechanism of the transporter. The pKa values of 3.6 for E290$^{7.38}$ in LeuT and 2.7 for D259$^{7.42}$ in Tyt1 in their crystal structure-like conformations indicate that they are primarily ionized (deprotonated) at physiological pH, in agreement with a previous study20. In both cases, the results pertain to the occluded state of the transporter in which E290 and D259 are deeply buried in the protein core and in complex with Na1. Analysis of the microenvironment around E290 shows that the titratable moiety is surrounded mostly by polar residues in addition to the Na^+ ion, which yields a hydrophilic microenvironment that is fairly typical for D or E21. This is reflected in the values, calculated as described in METHODS, of the interaction energy (w^{int}) and the transfer energy (Δw^{tr}) of −3 and 2 Kcal/mol, respectively; these contributions largely cancel each other out, and in the present case lead to only a modest lowering of the pKa value from its reference value of 4.4 in water. Thus, the fact that the transfer energy is > 0 shows that, in spite of the effect of Na^+, the microenvironment is still less hydrophilic than if it consisted entirely of water and hence the modification in pKa is small. Interestingly, the pKa value of E290 in the crystal structure-like LeuT model without Na^+ and substrate18 is 1.7 units above the reference value, as compared to 0.8 pKa units below the reference value when Na^+ is in the immediate vicinity of E290.

An additional, function-related alteration in pKa is caused by significant changes in the microenvironment of E290 that result from the adoption of the inward-facing conformation. Although the titratable groups of E290 (and D259) are still mostly buried in protein (~ 95 %), which shields them from the solvent, the structural rearrangement and the interactions of polar residues with a few isolated water molecules produce a significant change in the microenvironment of the acidic side chains. Thus, in the inward-facing conformation, the neighborhood of the buried acidic residues is composed of more hydrophobic residues than before the rearrangement to the inward-facing conformation (even the surrounding polar residues contribute mostly their hydrophobic portions to this environment). The net result is that the local environment around E290 is much more hydrophobic than in the LeuT crystal structure10, which increases the energy required for transferring the residue from water into the protein to 4.5 Kcal/mol. The interaction energy is −1.1 Kcal/mol, yielding a net gain of 3.4 Kcal/mol, which shifts the value of the pKa upwards (relative to the reference value) by 2.5 pH units, to 6.9.

DISCUSSION

Here we have demonstrated the existence of Na^+/substrate symport-mediated H^+ antiport by Cl^--independent members of the NSS family, a novel mechanistic finding for this class of membrane proteins. The ‘classical’ form of metabolic energy gradient across bacterial membranes, according to the chemiosmotic hypothesis of Mitchell22 is the protonmotive force (pmf). This driving force consists of an electrical membrane potential ($\Delta\Psi$) and a chemical proton gradient ($\Delta\mu_{H^+}$) across the bacterial plasma membrane. For many Na^+ dependent solute symport systems, such as members of the Solute:Sodium Symporter (SSS) family (e.g. PutP23 and hSGLT124), the Dicarboxylate/Amino Acid:Cation Symporter (DAACS) family (e.g. SdcS25), and the Bile Acid:Sodium Symporter (BASS) family (e.g. Abst26) $\Delta\mu_{H^+}$ contributes to the electrochemical force of $\Delta\tilde{\mu}_{Na^+}$–driven substrate symport due to its effect on $\Delta\Psi$. In striking contrast to this prototypical scheme for Na^+-coupled solute transport, however, we show here that $\Delta\mu_{H^+}$ directly acts *against* substrate transport catalyzed by the Cl^--independent NSS members Tyt1 and MhsT. Thus, detailed kinetic studies of Tyt1 in proteoliposomes, (Fig. 2&3), revealed that a negative $\Delta\mu_{H^+}$ is necessary to maximally stimulate Na^+-coupled substrate symport. In addition, our results in intact cells and Tyt1-containing proteoliposomes indicate that Na^+/substrate symport creates significant changes in the internal pH, consistent with internal alkalization stemming from H^+ export (Fig. 5).

In contrast to the Cl^--independent Tyt1-WT and MhsT-WT, the constructs in which the aspartate at position 7.38 (D259 and D263 in Tyt1 and MhsT, respectively) was mutated to asparagine, are Cl^--dependent and exhibit diminished dependence on the negative $\Delta\mu_{H^+}$. Thus, the Cl^--dependent members of the NSS family have neutral amino acids at position 7.38 or 7.42, whereas all Cl^--independent NSS members have a negatively charged amino acid at one of these positions (Supplementary Table 1). Together with our recent findings13, the results of the current work allow us to propose that the negatively charged amino acids located at position 7.38/7.42 are directly involved in H^+ translocation (Fig. 6a). The involvement of acidic amino acids in H^+ translocation has been suggested for H^+

translocating proteins, i.e. LacY27 and in the H^+-translocating F_1F_0 ATPase of *E. coli* (for review see28). Consequently, we interpret our results indicating that the conformational transitions associated with the transport cycle modulate the microenvironment of the charged residue and, in turn, alter its pKa, to suggest a facilitated protonation/deprotonation during the transport cycle.

Analysis of the significant pKa increase by > 3 units for E290 in LeuT and D259 in Tyt1 when comparing the inward-facing to the crystal structure-like conformation shows that E290 in LeuT and D259 in Tyt1 become protonated in the inward-facing conformations in which water molecules penetrate and modulate their local microenvironments. This is likely required in the inward facing state for the Na^+ and substrate-depleted transporter to facilitate movement to the outward facing configuration for the next cycle (Fig. 6 a). Such a proposed mechanism is supported by the finding that Tyr transport by Tyt1-WT is increased by 500% when the external pH is raised from pH 6.5 ($[H^+]$ = 0.316 μM) to pH 8.5 ($[H^+]$ = 0.003 μM) while the internal pH is maintained at pH 6.5 (Fig. 3c), thus generating a negative $\Delta\mu_{H^+}$. In contrast to the Cl^--dependent members of the NSS family, e.g., in GAT1 (Fig. 6 b) where reorientation of the transporter occurs with a neutral side chain at 7.38/7.42, in the Cl^--independent NSS members, as well as the Cl^--independent GAT1-S331E mutant13, the negative side chain of D or E at position 7.38 or 7.42 accepts an H^+ (or H_3O^+) due to the changes in the pKa. Reorientation appears to be the rate limiting step in the transport cycle, as judged by the dramatic effect of $\Delta\mu_{H^+}$ in stimulating turnover. However, substrate binding to the mutated Tyt1 variant, which lacks the vectorial component of Tyt1-mediated substrate translocation across the membrane, is essentially unaffected by pH (Fig. 4a).

Note however, that whereas Keynan & Kanner7, Hilgeman & Lu29, and Zomot *et al*.13 propose the coupled translocation of 1 GABA, 2 Na^+ and 1 Cl^- by GAT1, there is also evidence in GAT1 and DAT suggesting that under some conditions there is no net transport of Cl^- ("Cl^--cycling")30,31. In addition, Na^+/Cl^-/serotonin symport-coupled K^+ and/or H^+ antiport by SERT has been proposed32-34..

In spite of these observed differences, a unifying feature of the proposed mechanism for all NSS members is that the charge of the cotransported Na^+ ions must be compensated. Our findings point to the general conclusion that this is accomplished either by acidic groups in the protein (H^+ antiporting NSS members), or by the movable charge of the co-transported Cl^- (Cl^--dependent NSS members).

From a structural perspective (Fig. 7), [Au: ok to call out Figure 7 as a whole here, to avoid rearranging text about Fig. 7c and 7b below?] E290 in LeuT, a titratable residue, is closely associated with the Na^+ binding pocket and is in direct interactions with two Na1 site residues, T254 and N286 (Fig. 7a); conversely, as described in RESULTS, Na1 contributes significantly to the hydrophilic environment of E290, which, in combination with the Glu^--Na^+ electrostatic interaction renders E290 deprotonated at physiological pH. In turn, the rearrangement of the microenvironment in the absence of Na1 makes it less hydrophilic, destabilizing the deprotonated form of E290. Thus the Na^+ binding/dissociation and the E290 deprotonation/protonation events are likely to be closely associated in the transition between inward- and outward-facing conformations. In our well-equilibrated Tyt1 model,

similar orientation of D259 relative to the Na1 site is also observed, though D259 is one turn away from the aligned position of E290 in LeuT (Fig. 7c). Such immediate proximity of Na^+ and H^+ binding sites along their transport pathway is reminiscent of NhaA, an Na^+/H^+ antiporter35. Based on extensive simulation, Arkin *et al*. proposed that in NhaA, D164 is a Na^+ binding site and D163 controls the alternating access mechanism, which includes protonation/deprotonation events of both D163 and D164 and results in Na^+/H^+ antiport36 (Fig. 7b).

In terms of charge movements, Na^+/H^+ antiport is equivalent to the symport of Na^+/Cl^-. Interestingly, in the Cl^--dependent mammalian NSS the Cl^- site has been found as well to be close to the Na1 site13. We find that in our DAT model with embedded Na^+ and Cl^-[37], S321 and N353 consistently interact with both Na1 and Cl^- along the 16 ns equilibration trajectory (Fig. 7d). This evidence for direct coupling of Na^+ and H^+ (or Cl^-) binding suggests that the structural features surrounding E290 and the Na1 site of LeuT may indeed bring about the Na^+/H^+ antiport mechanism of Cl^--independent NSS revealed by this study.

The literature shows that the use of different solutions to achieving the same transport phenotype in closely related proteins (or in proteins in which an acidic amino acid (D or E) was replaced with a polar one (T or S)), is not to be unique to the NSS family. For example, replacement of D85 with T in the light-driven proton pump bacteriorhodopsin transformed the mutated bacteriorhodopsin into a chloride ion pump, which, like halorhodopsin, actively transports chloride ions in the direction opposite from the proton pump38.

Despite the opposite charge of the coupling ions, the NSS family of proteins shares a similar molecular mechanism if it is understood that a key step in the reaction cycle (Fig. 6) of NSS is the maintenance of an ionic counterbalance that compensates for the translocated Na^+.

METHODS

Expression of recombinant transport proteins

Tyt1 and MhsT were expressed in *E. coli* MQ614 [SVS1144 *mtr aroP tnaB271::*Tn5 *tyrP1 pheP::cat*]11 or *Lactococcus lactis* NZ9000 using pQ2 and pQmhsT or pNZ2 and pNZmhsT, respectively12. Mutations were introduced in the *tyt1* or *mhsT* genes according to the procedures described in the QuikChange® Site-Directed Mutagenesis Kit (Stratagene) using mutagenic oligonucleotides (Invitrogen) with pQ2 or pQmhsT as template. The following amino acid replacements were introduced in Tyt1 ($[D_{259}N_{260}A_{263}] \rightarrow [N_{259}S_{260}S_{263}]$) and MhsT ($D_{268} \rightarrow S_{268}$). All modifications were confirmed by DNA sequencing (Agencourt Bioscience Corp).

Purification, reconstitution and functional assays

Purification, resonctitution, and functional assays were performed as described12 (see also SUPPLEMENTARY METHODS online). Briefly, purified protein was reconstituted in pre-formed liposomes made of *E. coli* polar lipid extract and egg L-α-phosphatiylcholine (both Avanti) at a 2:1 (w/w) ratio. Protein activity was measured by means of transport studies in proteoliposomes and binding studies using the scintillation proximity assay (SPA) using Cu^{2+} chelate YSi scintillation SPA beads (GE Healthcare) in conjunction with the poly-His-

tagged recombinant proteins. 0.5 μg of purified and desalted protein were used per assay in assay buffer composed of Tris/Mes and Na-salt (equimolar replacement of Tris/Mes with Na-salts to obtain a total of 450 mM) and pH as indicated/20% glycerol/1 mM TCEP/0.1% n-dodecyl-β-D-maltopyranoside and the indicated concentration of $_{L}$-^{3}H-Tyr. For the determination of the dependence of the ion species/concentration on radioligand binding to the purified protein, the eluted protein fraction was desalted with Zeba® Desalt Spin Columns (Pierce) previously pre-equilibrated with 200 mM Tris/Mes, pH 7.5/20 % glycerol/1 mM TCEP/0.1% n-dodecyl-β-D-maltopyranoside.

Measurement of pH changes in intact *L. lactis* and proteoliposomes

L. lactis NZ9000 were cultivated and harvested as described above, washed and resuspend in 50 mM HEPES-K, pH 8.0. Incorporation of 1 μM 5-(and -6)-carboxyfluorescein diacetate succinimidyl ester (cFDASE; Invitrogen), which is subsequently hydrolyzed by esterases to 5 (and 6-)-carboxyfluorescein succinimidyl ester (cFSE) in the cytoplasm, was achieved by incubation for 15 min at 30 °C39. The suspension was washed and resuspend in 50 mM potassium phosphate buffer, pH 7.0, and 10 mM lactose was added for 30 min to eliminate non-conjugated cFSE. Free cFDASE was removed by washing the cells three times in 50 mM potassium phosphate buffer. For the determination of the internal pH changes within *L. lactis*, the cells were diluted to an optical density at 600 nM (OD_{600}) of 0.1 in 50 mM Tris/Mes, pH 7.5. The fluorescence intensity was measured at an excitation wavelength of 490 nm and excitation wavelength of 530 nM (at 5 nm slit widths). The effect of ligand-induced changes was tested by the addition of 20 mM NaCl and/or 10 μM Tyr after the recordings reached a stable baseline (routinely 200 s).

pH changes in proteoliposomes were measured by changes in pyranine fluorescence (excitation wavelength of 450 nm, excitation wavelength of 508 nM; 5 nm slit widths)40, 41. Pyranine-containing proteoliposomes were diluted into 5 mM potassium phosphate, pH 7.4 to a concentration of 4 μg protein/mL, and 20 mM NaCl and/or 10 μM Tyr were added after the fluorescence intensity was stable.

Data Analysis

All experiments were repeated at least in duplicate. Figures represent typical experiment, and, unless otherwise noted, data points represent the mean of a triplicate determination (n = 3) +/− S.D. Data fits of kinetic analyses were performed using non-linear regression algorithms in Sigmaplot (SPSS Inc., Chicago, IL) or Prism (GraphPad, San Diego, CA) and errors represent the S.E.M. of the fit.

pKa calculations

pKa calculations for particular amino acid residue side chains were performed according to the MM-SCP (Microenvironment Modulated-Screened Coulomb Potential) computational approach for calculating acid/base equilibria in proteins19. This method is based on expressing the protonation state of a titratable residue in a protein in terms of a thermodynamic cycle42, 43 and is described in detail in the SUPPLEMENTAL METHODS.

Supplementary Material

Refer to Web version on PubMed Central for supplementary material.

ACKNOWLEDGEMENTS

We thank Dr. Baruch Kanner for helpful discussion, Dr. Mary Ann Gawinovicz of the Columbia University Medical Center Protein Core Facility for the MALDI-TOF analysis of Tyt1, and Lynn Chung for technical assistance. Computations were performed on the Ranger at the Texas Advanced Computing Center (TG-MCB090022) and the computational infrastructure of the Institute for Computational Biomedicine at Weill Cornell Medical College. This work was supported by National Institutes of Health Grants DA022413 and DA17293 (JAJ), P01 DA012923 (HW), DA015170 (ELM), and K99 DA023694 (LS).

REFERENCES

1. Rudnick, G., editor. Mechanisms of biogenic amine neurotransmitter transporters. Humana Press Inc.; Totowa, New Jersey: 2002. p. 25-52.
2. Amara SG, Sonders MS. Neurotransmitter transporters as molecular targets for addictive drugs. Drug Alcohol Depend. 1998; 51:87–96. [PubMed: 9716932]
3. Iversen L. Neurotransmitter transporters and their impact on the development of psychopharmacology. Br J Pharmacol. 2006; 147(Suppl 1):S82–88. [PubMed: 16402124]
4. Gu H, Wall SC, Rudnick G. Stable expression of biogenic amine transporters reveals differences in inhibitor sensitivity, kinetics, and ion dependence. J Biol Chem. 1994; 269:7124–7130. [PubMed: 8125921]
5. Norregaard L, Gether U. The monoamine neurotransmitter transporters: structure, conformational changes and molecular gating. Curr Opin Drug Discov Devel. 2001; 4:591–601.
6. Torres GE, Gainetdinov RR, Caron MG. Plasma membrane monoamine transporters: structure, regulation and function. Nat Rev Neurosci. 2003; 4:13–25. [PubMed: 12511858]
7. Keynan S, Kanner BI. γ-Aminobutyric acid transport in reconstituted preparations from rat brain: coupled sodium and chloride fluxes. Biochemistry. 1988; 27:12–17. [PubMed: 3349023]
8. Wadiche JI, Amara SG, Kavanaugh MP. Ion fluxes associated with excitatory amino acid transport. Neuron. 1995; 15:721–728. [PubMed: 7546750]
9. Androutsellis-Theotokis A, et al. Characterization of a functional bacterial homologue of sodium-dependent neurotransmitter transporters. J Biol Chem. 2003; 278:12703–12709. [PubMed: 12569103]
10. Yamashita A, et al. Crystal structure of a bacterial homologue of Na^+/Cl^--dependent neurotransmitter transporters. Nature. 2005; 437:215–223. [PubMed: 16041361]
11. Quick M, et al. State-dependent conformations of the translocation pathway in the tyrosine transporter Tyt1, a novel neurotransmitter:sodium symporter from Fusobacterium nucleatum. J Biol Chem. 2006; 281:26444–26454. [PubMed: 16798738]
12. Quick M, Javitch JA. Monitoring the function of membrane transport proteins in detergent-solubilized form. Proc Natl Acad Sci U S A. 2007; 104:3603–3608. [PubMed: 17360689]
13. Zomot E, et al. Mechanism of chloride interaction with neurotransmitter:sodium symporters. Nature. 2007; 449:726–730. [PubMed: 17704762]
14. Loo DD, et al. Perturbation analysis of the voltage-sensitive conformational changes of the Na^+/glucose cotransporter. J Gen Physiol. 2005; 125:13–36. [PubMed: 15596535]
15. Goldberg NR, et al. Probing conformational changes in neurotransmitter transporters: a structural context. Eur J Pharmacol. 2003; 479:3–12. [PubMed: 14612133]
16. Beuming T, Shi L, Javitch JA, Weinstein H. A comprehensive structure-based alignment of prokaryotic and eukaryotic neurotransmitter/Na^+ symporters (NSS) aids in the use of the LeuT structure to probe NSS structure and function. Mol Pharmacol. 2006; 70:1630–1642. [PubMed: 16880288]
17. Quick M, Jung H. Aspartate 55 in the Na^+/proline permease of *Escherichia coli* is essential for Na^+-coupled proline uptake. Biochemistry. 1997; 36:4631–6. [PubMed: 9109673]

18. Shi L, et al. The mechanism of a neurotransmitter:sodium symporter--inward release of Na^+ and substrate is triggered by substrate in a second binding site. Mol Cell. 2008; 30:667–677. [PubMed: 18570870]
19. Mehler EL, Guarnieri F. A self-consistent, microenvironment modulated screened coulomb potential approximation to calculate pH-dependent electrostatic effects in proteins. Biophys J. 1999; 77:3–22. [PubMed: 10388736]
20. Forrest LR, et al. Identification of a chloride ion binding site in Na^+/Cl^-dependent transporters. Proc Natl Acad Sci U S A. 2007; 104:12761–112766. [PubMed: 17652169]
21. Pace CN, Grimsley GR, Scholtz JM. Protein ionizable groups: pK values and their contribution to protein stability and solubility. J Biol Chem. 2009; 284:13285–13289. [PubMed: 19164280]
22. Mitchell P. Molecule, group and electron translocation throught natural membranes. Biochem. Soc. Symp. 1962; 22:142–168.
23. Jung H, Tebbe S, Schmid R, Jung K. Unidirectional reconstitution and characterization of purified Na^+/proline transporter of *Escherichia coli*. Biochemistry. 1998; 37:11083–11088. [PubMed: 9693004]
24. Quick M, Wright EM. Employing *Escherichia coli* to functionally express, purify, and characterize a human transporter. Proc Natl Acad Sci U S A. 2002; 99:8597–8601. [PubMed: 12077304]
25. Hall JA, Pajor AM. Functional reconstitution of SdcS, a Na^+-coupled dicarboxylate carrier protein from Staphylococcus aureus. J Bacteriol. 2007; 189:880–885. [PubMed: 17114260]
26. Sun AQ, et al. Identification of functionally relevant residues of the rat ileal apical sodium-dependent bile acid cotransporter. J Biol Chem. 2006; 281:16410–16418. [PubMed: 16608845]
27. Smirnova IN, Kasho V, Kaback HR. Protonation and sugar binding to LacY. Proc Natl Acad Sci U S A. 2008; 105:8896–8901. [PubMed: 18567672]
28. Capaldi RA, Aggeler R. Mechanism of the F_1F_0-type ATP synthase, a biological rotary motor. Trends Biochem Sci. 2002; 27:154–160. [PubMed: 11893513]
29. Hilgemann DW, Lu CC. GAT1 (GABA:Na^+:Cl^-) cotransport function. Database reconstruction with an alternating access model. J Gen Physiol. 1999; 114:459–475. [PubMed: 10469735]
30. Loo DD, et al. Role of Cl- in electrogenic Na^+-coupled cotransporters GAT1 and SGLT1. J Biol Chem. 2000; 275:37414–37422. [PubMed: 10973981]
31. Erreger K, Grewer C, Javitch JA, Galli A. Currents in response to rapid concentration jumps of amphetamine uncover novel aspects of human dopamine transporter function. J Neurosci. 2008; 28:976–89. [PubMed: 18216205]
32. Rudnick G, Nelson PJ. Platelet 5-hydroxytryptamine transport, an electroneutral mechanism coupled to potassium. Biochemistry. 1978; 17:4739–4742. [PubMed: 728383]
33. Rudnick G, Clark J. From synapse to vesicle: the reuptake and storage of biogenic amine neurotransmitters. Biochim Biophys Acta. 1993; 1144:249–63. [PubMed: 8104483]
34. Keyes SR, Rudnick G. Coupling of transmembrane proton gradients to platelet serotonin transport. J Biol Chem. 1982; 257:1172–1176. [PubMed: 7056713]
35. Hunte C, et al. Structure of a Na^+/H^+ antiporter and insights into mechanism of action and regulation by pH. Nature. 2005; 435:1197–1202. [PubMed: 15988517]
36. Arkin IT, et al. Mechanism of Na^+/H^+ antiporting. Science. 2007; 317:799–803. [PubMed: 17690293]
37. Guptaroy B, et al. A Juxtamembrane mutation in the N-terminus of the dopamine transporter induces preference for an inward-facing conformation. Mol Pharmacol. 2009; 75:514–524. [PubMed: 19098122]
38. Sasaki J, et al. Conversion of bacteriorhodopsin into a chloride ion pump. Science. 1995; 269:73–5. [PubMed: 7604281]
39. Breeuwer P, Drocourt J, Rombouts FM, Abee T. A novel method for continuous determination of the intracellular pH in bacteria with the internally conjugated fluorescent probe 5 (and 6-)-carboxyfluorescein succinimidyl ester. Appl Environ Microbiol. 1996; 62:178–183. [PubMed: 16535209]

40. Kano K, Fendler JH. Pyranine as a sensitive pH probe for liposome interiors and surfaces. pH gradients across phospholipid vesicles. Biochim Biophys Acta. 1978; 509:289–299. [PubMed: 26400]

41. Indiveri C, Tonazzi A, Stipani I, Palmieri F. The purified and reconstituted ornithine/citrulline carrier from rat liver mitochondria: electrical nature and coupling of the exchange reaction with H^+ translocation. Biochem J. 1997; 327(Pt 2):349–355. [PubMed: 9359400]

42. Warshel A. Calculations of enzymatic reactions: calculations of pKa, proton transfer reactions, and general acid catalysis reactions in enzymes. Biochemistry. 1981; 20:3167–3177. [PubMed: 7248277]

43. Bashford D, Karplus M. pKa's of ionizable groups in proteins: atomic detail from a continuum electrostatic model. Biochemistry. 1990; 29:10219–10225. [PubMed: 2271649]

44. Screpanti E, Hunte C. Discontinuous membrane helices in transport proteins and their correlation with function. J Struct Biol. 2007; 159:261–7. [PubMed: 17350860]

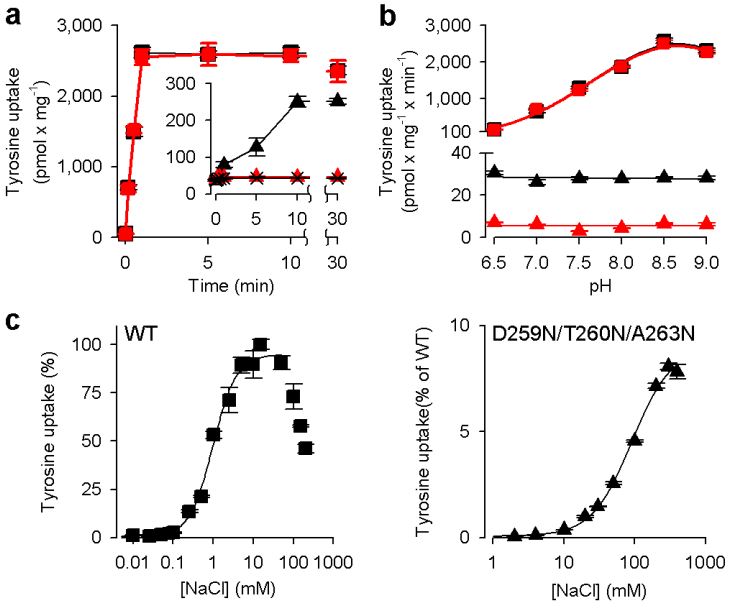

Figure 1.

Tyrosine uptake by intact *E. coli* cells. **a**) Time course of 1 μM ^{3}H-Tyr transport by *E. coli* MQ614 harboring given Tyt1 variants (wild-type, WT, squares; D259N/A263N, triangles) in the presence of NaCl (black symbols) or Na-gluconate (red symbols) at pH_{out} of 8.5. Uptake by Tyt1 wild-type (WT, squares) was assayed in the presence of 10 mM NaCl or Na-gluconate, whereas the salt concentration was increased to 100 mM for uptake measurements involving Tyt1-D259N/A263N (*inset*). *E. coli* MQ614 transformed with a plasmid devoid of *tyt1* served as control (X, depicting the data points obtained in 100 mM NaCl which were virtually identical to those in 10 mM NaCl or Na-gluconate, or 100 mM Na-gluconate). **b**) pH dependence of specific Tyr uptake (1 μM ^{3}H-Tyr; 1 min) by intact *E. coli* MQ614 containing Tyt1-WT (○;○) or -D259N/A263N (▲;▲) in the presence of NaCl (black symbols) or Na-gluconate (red symbols). Salt concentrations were identical to those described in panel a. **c**) Stimulation of Tyr transport (1 μM final concentration) by intact *E. coli* MQ614 harboring Tyt1-WT (left panel, ○) or Tyt1-D259N/T260N/A263N (right panel, ▲) by increasing the NaCl concentration (pH_{out} = 8.5). All experiments were repeated at least in duplicate and the panels depict representative experiments showing the means ± S.E.M of triplicate determinations.

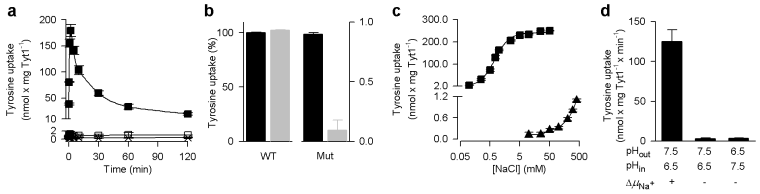

Figure 2.

Tyrosine uptake in proteoliposomes containing purified recombinant Tyt1. **a**) The time course of 1 μM ^{3}H-Tyr uptake in the presence (○) or absence (□) of 25 mM NaCl. Liposomes devoid of Tyt1 served as control (X). **b**) Initial rate of 1 μM ^{3}H-Tyr in proteoliposomes containing Tyt1-WT (left panel) or -D259N/T260N/A263N (Mut, right panel) measured in the presence of NaCl (black bars) or Na-gluconate (light gray bars). Na^{+}-salt concentrations were 25 and 200 mM for Tyt1-WT and -D259N/T260N/A263N, respectively. Data were normalized with regard to WT-mediated transport in the presence of NaCl. **c**) Stimulation of 1 μM ^{3}H-Tyr transport in proteoliposomes containing Tyt1-WT (○)12 or Tyt1-D259N/T260N/A263N (▲) by increasing the NaCl concentration. Uptake experiments shown in **a-c** were performed with proteoliposomes with pH_{in} = 6.5 and pH_{out} = 8.5 (generation of a negative $\Delta\mu_{H^+}$). **d**) Tyt1-mediated tyrosine transport is strictly dependent on $\Delta\mu_{Na^+}$. Uptake of 1 μM ^{3}H-Tyr was measured in the presence of 25 mM external NaCl (in the absence of valinomycin) with Tyt1-WT-containing proteoliposomes that were prepared in the presence (no $\Delta\mu_{Na^+}$) or absence (inwardly-directed $\Delta\mu_{Na^+}$) of 25 mM NaCl . An inwardly- or outwardly-directed $\Delta\mu_{H^+}$ in the absence of $\Delta\mu_{Na^+}$ resulted in uptake activity comparable to that in control liposomes. Experiments in a, b, and d were repeated at least in duplicate and the panels depict representative experiments with the means ± S.E.M of triplicate determinations; data in **c** are shown as the mean ± S.E.M of triplicate measurements.

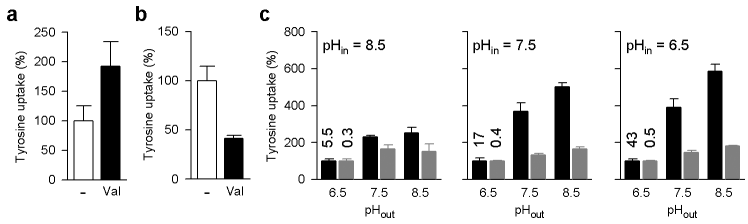

Figure 3.

Influence of membrane potential and pH gradient on Tyt1-mediated transport. Effect of an **a**) inwardly- or **b**) outwardly-directed membrane potential ($\Delta\Psi$) on the initial rates of Tyt1-WT-mediated transport. **a**) $\Delta\mu_{Na^+}$-dependent (25 mM NaCl) uptake of 1 μM ^{3}H-Tyr was measured in the presence (black bars) and absence (white bars) of valinomycin at pH_{in} = pH_{out} = 6.5. **b**) $\Delta\mu_{Na^+}$- and $\Delta\mu_{H^+}$-dependent (25 mM NaCl; pH_{in} = 6.5; pH_{out} = 8.5) uptake of 1 μM ^{3}H-Tyr was measured in Tyt1-WT proteoliposomes containing 10 mM KP_i in the presence of 50 mM external KP_i in the presence or absence of valinomycin. Data in **a** and **b** were normalized with regard to the uptake activity in the absence of 1 μM valinomycin (Val). **c)** Na^+-dependent Tyr transport (1-minute measurements) in proteoliposomes containing Tyt1-WT (black bars) and -D259N/T260N/A263N (gray bars) in response to $\Delta\mu_{H^+}$ (variation of pH_{in} and pH_{out}). Uptake of 1 μM ^{3}H-Tyr was measured in the presence of 25 mM (WT) or 200 mM NaCl (D259N/T260N/A263N) and 1 μM valinomycin. Data for Tyt1-WT and -D259N/T260N/A263N were normalized with regard to their respective transport rates at pH_{out} = 6.5 at each pH_{in}. The actual rates (in pmol × mg^{-1} × min^{-1}) for WT and the mutant are shown above the corresponding bars. All experiments were repeated at least in duplicate and the panels depict representative experiments with the means ± S.E.M of triplicate determinations.

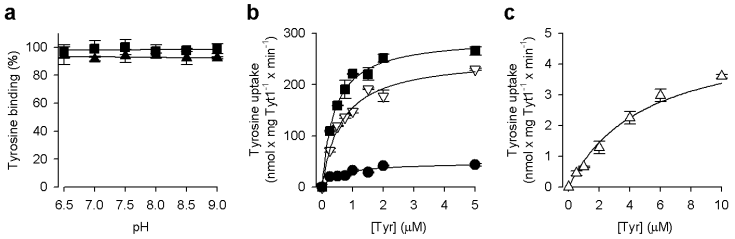

Figure 4.

Substrate kinetics of Cl^- dependent and independent Tyt1 variants. **a**) Equilibrium binding of 1 μM ^{3}H-Tyr by 1 μg of purified Tyt1-WT (○) and -D259N/T260N/A263N (▲) was assayed in the presence of 150 mM NaCl at different pH. Results were normalized to the data of Tyt1-WT. **b**) Na^+-dependent (25 mM) Tyr transport in Tyt1-WT-containing proteoliposomes (pH_{in} = 6.5) at different external pH (pH_{out} = 6.5, ●; pH_{out} = 7.5, ▽; pH_{out} = 8.5, ○). **c**) Tyrosine transport in proteoliposomes containing Tyt1-D259N/T260N/A263N (pH_{in} = 6.5, pH_{out} = 8.5) in the presence of 200 mM NaCl. Data points are shown as the mean ± S.E.M of triplicate measurements in representative experiments which were used for the determination of the kinetic constants shown ± S.D. of the fit.

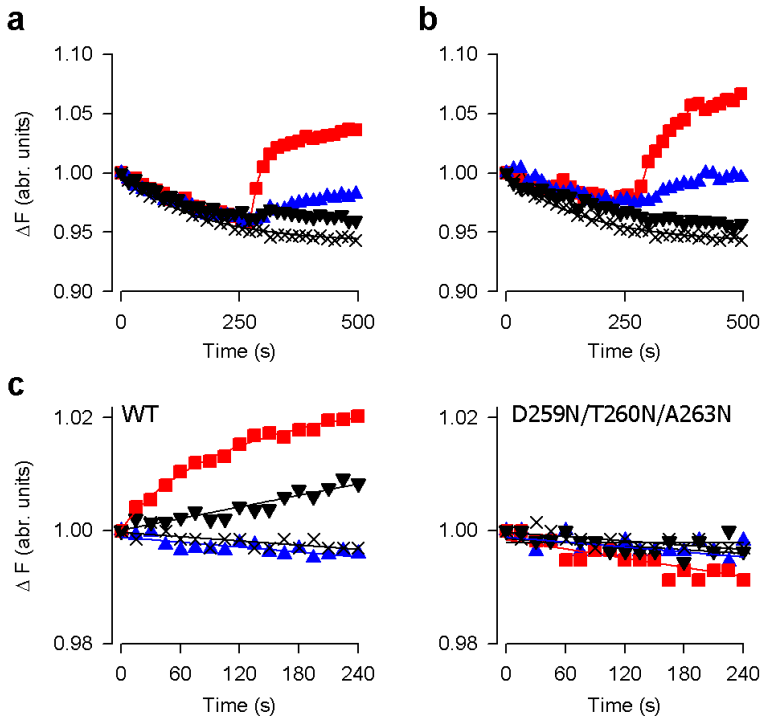

Figure 5.

Na^+/substrate coupled H^+ antiport. Ligand-induced changes in the cFSE fluorescence intensity ratio were measured in *L. lactis* NZ9000 expressing the recombinant *tyt1* (**a**) or *mhsT* (**b**) gene upon the addition of 20 mM NaCl (▲), 20 μM Tyr (▼), or 20 mM NaCl/20 μM Tyr (○). *L. lactis* NZ9000 (with control plasmid) served as a control and was tested with 20 mM NaCl/20 μM Tyr (x), which gave virtually identical results to the control with the individual substrates. **c**) Pyranine fluorescence measurements in proteoliposomes containing Tyt1-WT (left panel) and –D259N/T260N/A263N (right panel) upon the addition of 20 mM NaCl (▲), 20 μM Tyr (▼), or both ligands (○). Empty liposomes served as control for all conditions; for clarity only the fluorescence changes after the addition of 20 mM NaCl/20 μM Tyr are shown (x) – these were not different from the control with the individual substrates or no substrate added. The panels depict representative experiments with data points from individual determinations.

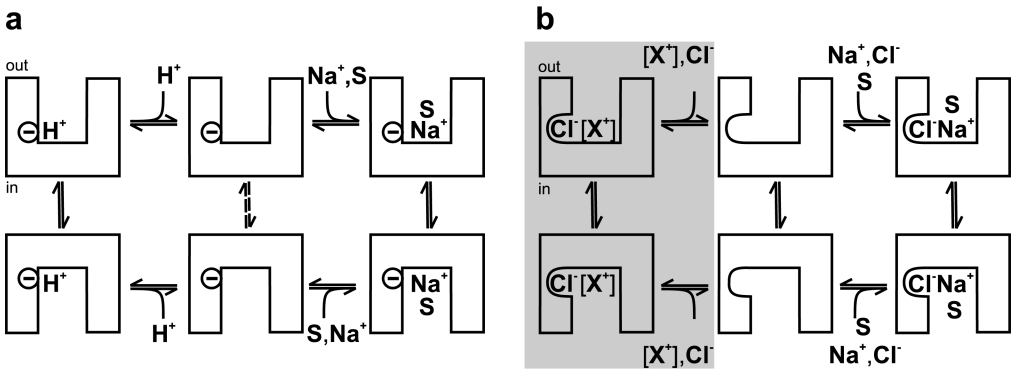

Figure 6.

Schematic representation of the NSS transport cycle. **a**) In the H^+-dependent NSS members a negative charge in the transporter compensates the positive charge of the cotransported Na^+. This negative charge is compensated by H^+ in the return step of the empty transporter resulting in net H^+ efflux. The broken arrows between the outward- and inward-facing empty transporter indicate a potential slow return step without H^+ efflux. **b**) Compensation of the charge of cotransported Na^+ by the moveable charge of Cl^- in the Cl^--dependent NSS members. The model takes into account net Cl^- influx7, 13 (non-shaded area) as well as "Cl^--cycling"30, 31 and cation ($[X^+]$) efflux32-34 (gray shaded area). This schematic representation is not intended to convey a specific stoichiometry, the sequence of binding/unbinding events, or the relative rates of the transitions (indicated by equilibrium arrows).

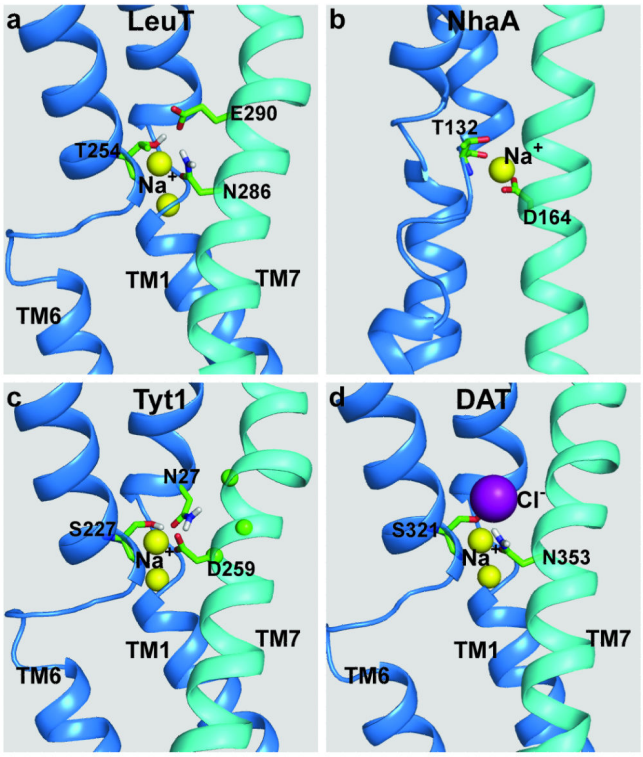

Figure 7.

The proximities of Na^+ and H^+/Cl^- binding sites in Na^+/H^+ antiport and Na^+/Cl-symport. **a**) In the LeuT structure, the deprotonated E290 forms H-bonds with two Na1 binding residues, T254 and N286. The Na1 binding site is located in the unwound regions of TM1 and TM6. **b**) In the NhaA structure, the Na^+ binding site is likely to be D164 and the protonation/deprotonation of D164 has been proposed to be involved in proton translocation36. For the purpose of illustration, a Na^+ ion is manually placed between T132 and D164, which are also close to unwound regions of two TMs44. **c**) The disposition of the negative charged D259 in our LeuT-based Tyt1 homology model is similar to that of LeuT and forms H-bond to two Na1 binding residues. The Cα atoms of the mutated residue positions of D259N/T260N/A263N mutant are shown as small spheres. **d**) In our LeuT-based dopamine transporter (DAT) homology model, the negatively charged Cl^- ion forms stable interactions with Na^+-binding residues. Thus the negative charge provided by either Asp/Glu or Cl^- is favored around Na^+ binding site.